Proceedings of the Canadian Society for Mechanical Engineering International Congress 2021
CSME Congress 2021
June 27-30, 2021, Charlottetown, PE, Canada

Research on Path-Tracking Control of Articulated Vehicle with a trailer Based on Advanced Model Prediction Control Strategy

Leilei Liu[1], Baohua Wang[1*], Yuping He[2]
[1]School of Vehicle Engineering, Hubei University of Automotive Technology, Shiyan,China, *Email:wbhbenz@126.com
[2]Department of Automotive and Mechatronics Engineering, University of Ontario Institute of Technology, Oshawa, Canada

Abstract—To improve the path-tracking ability and road adaptability for articulated vehicle with a trailer, this paper proposes an advanced path-tracking strategy, which is designed using the model predictive control method and an optimal curvature preview control technique. Firstly, a linear vehicle model was generated and its fidelity was verified. Then the model predictive controller was designed and used to reduce the lateral tracking error in curved path negotiations, and the optimal curvature preview control strategy was designed to improve the driving stability in straight road operation. Finally, a co-simulation platform based on Trucksim and Simulink software was built, and co-simulations were carried out under the double lane change and the single lane change maneuvers at different vehicle speeds. Simulation results show that the proposed path-tracking controller exhibits better performance than the optimal preview controller. The path-tracking ability and the driving stability are also excellent in the whole driving process for the single-trailer articulated vehicle.

Keywords: articulated heavy vehicle; model prediction control; optimal curvature preview control; track-following performance.

I. INTRODUCTION

Intelligent driving technology has gradually become a research hotspot in recent years, and the path-tracking control is one of key technologies for intelligent driving vehicle [1][2]. At present, studies on intelligent driving technology about passenger cars has been relatively mature, but for the articulated heavy vehicles (AHVs), due to its large sizes and big masses, the path-tracking control strategy for the traditional heavy vehicle is not suitable for the AHVs, and will lead to worse effects. Because of the great significance on the path-tracking ability and stability of AHVs, so, this research focuses on driver model design for AHV path-tracking control strategies.

MacAdam has proposed an optimal preview driver model [3][4]. The driver model calculated the required steering wheel angle according on the weighted square error between the target lateral position and the output lateral position of the continuous linear system, which can accurately track the target trajectory. But there is no control over the yaw angle of the vehicle. On this basis, Ungorn et al established a driver model considering the yaw angle, which has been used for passenger car closed-loop dynamic simulation [5]. Attempts have also been made to design driver models for AHVs [6][7].

Paolo Falcome et al. generated a four-wheel vehicle model and its simplified bicycle model, using model predictive controller (MPC) while braking or steering [8], so the path-tracking ability was greatly improved for the four-wheel passenger car. However, the control model cannot be directly applied to AHVs because of their inherent vehicle structures of single-unit vehicles. Hode et al designed a linear quadratic regulator (LQR) for the path-tracking of robot, but the lateral error was too large at the intersection of the straight line segment and the curve segments [9]. Salmon et al designed a nonlinear MPC controller for the agricultural vehicle, but the tracking error is still big at the road small curvature section [10]. Wu et al proposed a MPC controller based on lateral displacement error, aiming to address the path-tracking problem of AHVs [11], simulation results showed that the path-tracking ability is better, but there still existed a certain tracking error during the transition from a straight line segment to the curve segment. The kinematics model does not consider the dynamic constraints of AHV, so it can only be applied to the low speed driving cycle. In the middle or high-speed operations, the dynamics model must be built and applied for the AHVs.

To enhance the road adaptability of AHVs, this paper generates a single track yaw-plane model to represent an articulated vehicle with a trailer, and designs a path-tracking controller combining the MPC for curved path negotiation and the optimal curvature preview controller (OCPC) for straight road operation. The aim of MPC is to minimize the lateral tracking error in the curve segment, so that the tracking effect of AHVs is the best, and the control variable is constrained to avoid the folding phenomenon; the OCPC in the straight segment is to make the AHVs have a better lateral stability. Through the coordination of the two control strategies, the path-tracking ability and the driving stability are significantly improved for the AHVs under varied path geometric conditions.

II. VEHICLE MODEL AND VALIDATION

A. AHV Vehicle Modelling

As shown in Fig.1, the simplified vehicle model is mainly used to design the MPC controller as an ideal predictive model of AHVs. The model considers three degrees of

Fund Program：Natural Science Foundation of China (52072116) ; Key R&D Project of Hubei Province (2020BAB141) ;
About the author: Leilei Liu (1996-),male, from Jincheng, Shanxi, graduate student, engaged in research on driver model of articulated heavy vehicles. E-mail: 861415886@qq.com
Corresponding author: Baohua Wang, male, Professor, Ph.D., Research direction: Vehicle Dynamics and Control. E-mail:wbhbenz@126.com

freedom: the lateral movement of the tractor, the yaw movement of the tractor, and the yaw movement of the trailer. The simplified model satisfies the following assumptions [12][13]:

(1) Driving on a flat road, ignoring vertical movement;
(2) Ignoring the influence of aerodynamics;
(3) Ignoring the effects of suspension movements;
(4) Linearizing lateral tire dynamics;
(5) Only the front wheel of the tractor being steerable;
(6) Forward speed being constant.

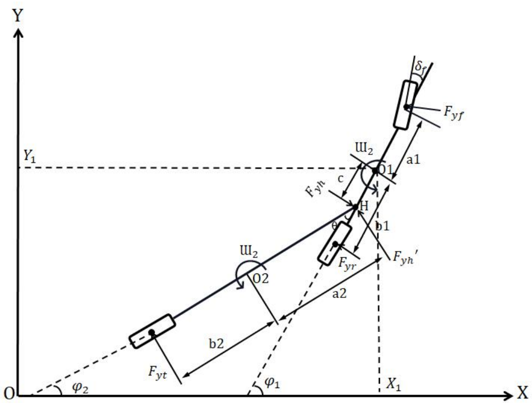

Fig 1. The simplified model for AHV Vehicle

The lateral dynamics equation of tractor is

$$m_1\ddot{y}_1 = k_f\alpha_f\cos\delta_f + k_r\alpha_r - F_{yh} \tag{1}$$

The lateral dynamics equation of trailer is

$$m_2\ddot{y}_2 = k_t\alpha_t + F_{yh}\cos\theta \tag{2}$$

The yaw dynamics equation of tractor is

$$I_{z1}\ddot{\varphi}_1 = a_1k_f\alpha_f\cos\delta_f - b_1k_r\alpha_r + cF_{yh} \tag{3}$$

The yaw movement equation of trailer is

$$I_{z2}\ddot{\varphi}_2 = a_2F_{yh}\cos\theta - b_2k_t\alpha_t \tag{4}$$

and the following constraints are met for the tractor and the trailer,

$$\theta = \varphi_1 - \varphi_2, \dot{x}_1 = \dot{x}_2, F_{yh} = F_{yh}^{'} \tag{5}$$

where, F_{yh} is lateral force at the articulated point. The tire slip angle and the lateral acceleration are described as,

$$\begin{aligned}
\alpha_f &= \frac{\dot{y}_1 + a_1\dot{\varphi}_1}{\dot{x}_1} - \delta_f \\
\alpha_r &= \frac{\dot{y}_1 - b_1\dot{\varphi}_1}{\dot{x}_1} \\
\alpha_t &= \frac{\dot{y}_2 - b_2\dot{\varphi}_2}{\dot{x}_2} = \frac{\dot{y}_1 - c\dot{\varphi}_1 - (a_2+b_2)\dot{\varphi}_2}{\dot{x}_2} + \theta \\
\ddot{y}_1 &= \dot{y}_1 + \dot{x}_1\dot{\varphi}_1 \\
\ddot{y}_2 &= \dot{y}_1 + \dot{x}_1\dot{\varphi}_1 - c\ddot{\varphi}_1 - a_1\ddot{\varphi}_2
\end{aligned} \tag{6}$$

where φ_1, and φ_2 are yaw angle of tractor and trailer, θ is articulation angle between tractor and trailer, α_f is slip angle of the front axle of the tractor, α_r is slip angle of the rear axle of the tractor, α_t is slip angle of the trailer axle, δ_f tractor front-wheel steering wheel.

Considering the relationship between the body coordinate system and the vehicle coordinate system, we can get:

$$\begin{aligned}
X_1 &= \dot{x}_1\cos\varphi_1 - y_1\sin\varphi_1 \\
Y_1 &= \dot{x}_1\sin\varphi_1 + \dot{y}_1\cos\varphi_1
\end{aligned} \tag{7}$$

where, x_1, y_1, x_2, y_2 are longitudinal and lateral position in the vehicle coordinate system of tractor and trailer, X_1, Y_1 are longitudinal and lateral position in the inertial coordinate system of tractor.

Convert the above differential equation into a state space expression:

$$\begin{aligned}
\dot{\chi} &= A\chi + Bu \\
\eta_{dyn} &= C\chi
\end{aligned} \tag{8}$$

The variable and matrices A, B and C are as follows:

$$\chi = \begin{bmatrix}\dot{y}_1 & \dot{\varphi}_1 & \dot{\varphi}_2 & \theta & \varphi_1 & Y_1\end{bmatrix}^T, u = \delta_f, \eta_{dyn} = \begin{bmatrix}\varphi_1 & Y_1\end{bmatrix}^T$$

$$E = \begin{bmatrix}k_f & a_1k_f & 0 & 0\end{bmatrix}^T,\ B = P^{-1}E,\ A = P^{-1}F$$

$$P = \begin{bmatrix}
m_1+m_2 & -m_2c & -m_2a_2 & 0 & 0 & 0 \\
-m_2c & I_{z1}+m_2c^2 & m_2a_2c & 0 & 0 & 0 \\
-m_2a_2 & m_2a_2c & I_{z2}+m_2{a_2}^2 & 0 & 0 & 0 \\
0 & 0 & 0 & 1 & 0 & 0 \\
0 & 0 & 0 & 0 & 1 & 0 \\
0 & 0 & 0 & 0 & 0 & 1
\end{bmatrix}$$

$$F = \begin{bmatrix}
\frac{k_f+k_r+k_t}{v_x} & \frac{a_1k_f-b_1k_r-ck_t-m}{v_x} & \frac{k_t(a_2+b_2)}{v_x} & k_t & 0 & 0 \\
\frac{k_fa_1-k_rb_1-k_tc}{v_x} & \frac{k_f{a_1}^2+k_r{b_1}^2+k_tc^2+m_2c}{v_x} & \frac{k_tc(a_2+b_2)}{v_x} & -k_tc & 0 & 0 \\
\frac{-k_t(a_2+b_2)}{v_x} & \frac{k_tc(a_2+b_2)+m_2a_2}{v_x} & \frac{k_t(a_2+b_2)^2}{v_x} & -k_t(a_2+b_2) & 0 & 0 \\
0 & 1 & -1 & 0 & 0 & 0 \\
0 & 1 & 0 & 0 & 0 & 0 \\
1 & 0 & 0 & 0 & v_x & 0
\end{bmatrix}$$

$$C = \begin{bmatrix} 0 & 0 & 0 & 0 & 0 & 0 \\ 0 & 0 & 0 & 0 & 0 & 0 \\ 0 & 0 & 0 & 0 & 0 & 0 \\ 0 & 0 & 0 & 0 & 0 & 0 \\ 0 & 0 & 0 & 0 & 1 & 0 \\ 0 & 0 & 0 & 0 & 0 & 1 \end{bmatrix}$$

Table 1 lists the basic parameters of the AHVs.

TABLE 1: The Vehicle Basic Parameters and Values

Symbol	Description	value
m_1	Whole mass of tractor (kg)	8450
m_{load}	Whole mass of trailer (kg)	30000
m_2	Whole payload (kg)	37255
a_1	Longitudinal distance between the front axle and the sprung mass CG of the tractor (m)	1.385
b_1	Longitudinal distance between the sprung mass CG of the tractor and the rear axle (m)	4.25
a_2	Longitudinal distance between the articulated point and the sprung mass CG of the trailer (m)	5.5
b_2	Longitudinal distance from the sprung mass CG of the trailer to the trailer axle (m)	4.72
c	Longitudinal distance from the sprung mass CG of the tractor to the articulated point (m)	4.25
k_f	Combined cornering stiffness of the tires of the front axle on the tractor (N/rad)	-135010
k_r	Combined cornering stiffness of the tires of the rear axle on the tractor (N/rad)	-477620
k_t	Combined cornering stiffness of the tires of the axle on the trailer (N/rad)	-550360
I_{z1}	Yaw moment of inertia of the tractor,measured about its whole mass CG (kgm^2)	20610
I_{z2}	Yaw moment of inertia of the trailer,measured about its whole mass CG (kgm^2)	700502

B. Model validation

To ensure the consistent response between the generated linear model and the nonlinear Trucksim model, the fishhook test and the step input test are carried out under the condition of 40km/h and the ground adhesion coefficient 0.85. The coincidence is defined to describe the accuracy of the linear model relative to the nonlinear Trucksim model in the steady state. The definition is as follows:

$$coincidence = 1 - \frac{|linear - nonlinear|}{nonlinear} \quad (9)$$

a. Fishhook test

Simulation conditions are specified as follows: steering wheel angle input is shown in Fig 2(a), and the amplitude is 300deg. The simulation results of transient yaw rate and lateral acceleration are shown in Fig 2(b)-Fig 2(c).

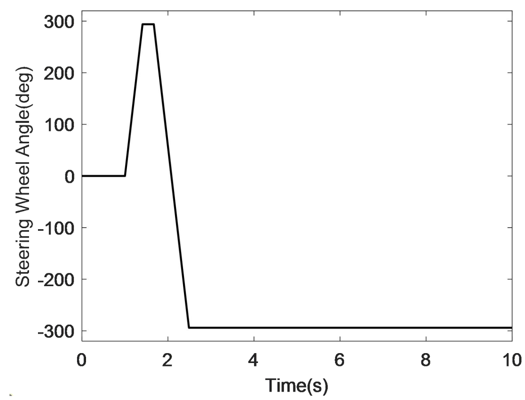

(a) Input of Fishhook Test

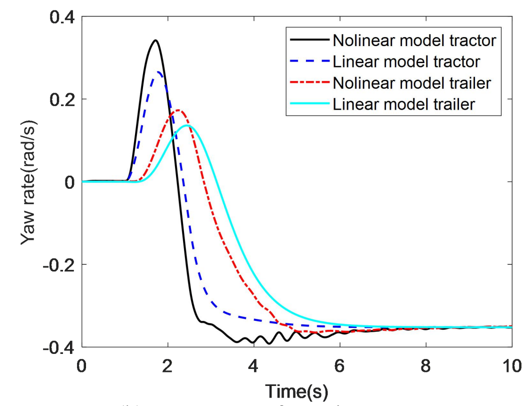

(b) Response of transient yaw rate

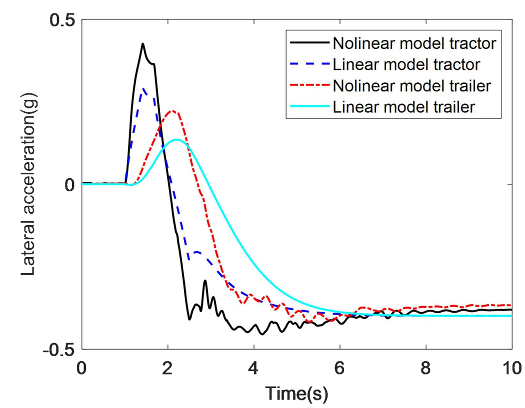

(c) Response of transient lateral acceleration

Fig 2. Transient response characteristics of the two vehicle models under fishhook test

It can be seen from Fig 2 that the response characteristic curves of the two models are close. The coincidence of the yaw rate is above 95%, and the coincidence of lateral acceleration is above 90% for the two vehicle models.

b. Step Input Test

Simulation conditions are set as follows: steering wheel angle input is shown in Fig 3(a), and the amplitude is 180deg. The response characteristics of yaw rate and lateral acceleration are shown in Fig 3(b)-Fig 3 (c).

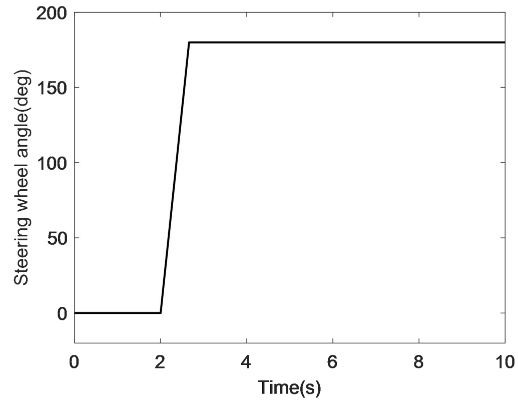

(a) Angular Step Input of steering wheel

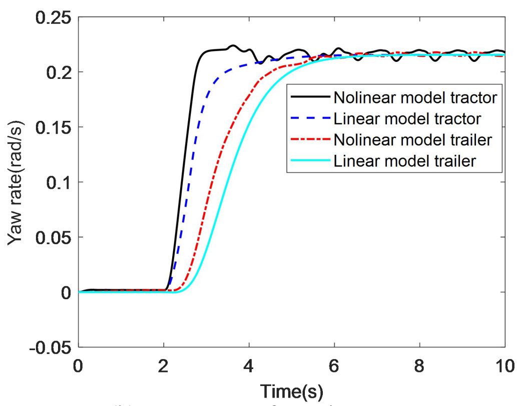

(b) Response of transient yaw rate

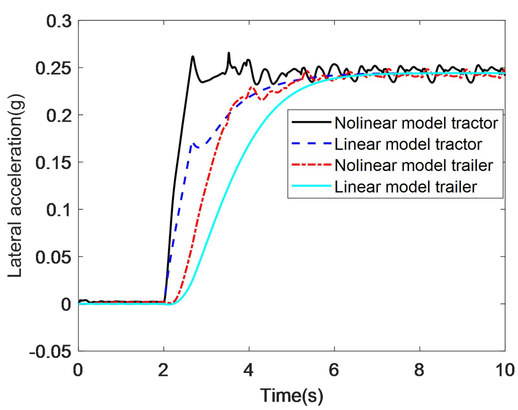

(c) Response of transient lateral acceleration

Fig 3. Transient response characteristics under step Input condition

As seen in Fig 3, when the steering wheel is suddenly turned from 0 to 180 deg at 2th second, the nonlinear model immediately responses and fluctuates at the steady state value. However, the linear vehicle model ignores factors such as suspensions etc., it is relatively small for the fluctuation of response characteristic curves. The coincidences between the yaw rate and the lateral acceleration are above 95% for the two vehicle models.

To sum up, it can be seen that the response characteristics of the two vehicle models have reached more than 90%, so the established linear vehicle model is accurate and meets the research requirements.

III. CONTROLLER DESIGN

MPC uses a linear dynamic model as a predictive model. The lateral movement control of AHVs on the reference path is regarded as a constrained optimal control problem, and the optimal solution can be obtained. As shown in Fig 4, a new path-tracking controller, which combines the merits of MPC and OCPC, is designed in this paper [14].

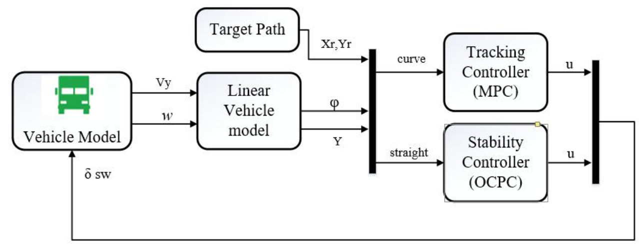

Fig 4. The new road-following controller for the AHVs

When the AHV tracks curve roads, the MPC is selected and applied to the vehicle, and the real-time optimization is used to reduce the lateral tracking error. While the AHV enters the straight road, the OCPC is selected, and the preview time can be adjusted by the driving speed.

A. Design of model predictive controller on curve road

When the AHV enters a curve from a straight, it is necessary to reduce path-tracking error as soon as possible. The MPC predicts the output according to the current state, and continuously updates the control commands to eliminate path-tracking errors. The model predictive control strategy is designed as follows [15].

a. Establishment of prediction equation

To design the model predictive controller, equation (8) is discretized by using the forward Euler method as:

$$\dot{\chi}(k) = \frac{\chi(k+1) - \chi(k)}{T} = A(k)\chi(k) + B(k)u(k) \tag{10}$$

$$\chi(k+1) = (I + TA(k))\chi(k) + TB(k)u(k) \tag{11}$$

where, I is the 6-order unit matrix, and T is the sampling time.

Furthermore, the equation (11) is transformed into:

$$\xi(k+1 \mid t) = \widetilde{A}_{k|t}\xi(k \mid t) + \widetilde{B}_{k|t}\Delta u(k \mid t) \tag{12}$$

$$\eta(\mathrm{k} \mid t) = \widetilde{C}_{k,t}\xi(k \mid t) \tag{13}$$

where, ξ Is the current state vector, Δ u is the current control increment, I_m is the m-order unit matrix, m is the number of state variables, n is the number of control variables.

$$\xi(k\mid t)=\begin{bmatrix}\chi(k\mid t)\\ u(k-1\mid t)\end{bmatrix},\quad \widetilde{A}_{k,t}=\begin{bmatrix}A(k\mid t) & B(k\mid t)\\ 0_{m\times n} & I_m\end{bmatrix},$$

$$\widetilde{B}_{k,t}=\begin{bmatrix}B(k\mid t)\\ I_m\end{bmatrix},\quad \widetilde{C}_{k,t}=\begin{bmatrix}C(k\mid t) & 0\end{bmatrix}.$$

At this time, the prediction equation [16] is expressed as:

$$Y(k\mid t)=\psi_{k,t}\xi(k\mid t)+\Phi_{k,t}\Delta u(k\mid t) \tag{14}$$

where, N_p is the prediction horizon, N_c is the control horizon.

$$Y(k\mid t)=\begin{bmatrix}\eta(k+1\mid t)\\ \eta(k+2\mid t)\\ \eta(k+3\mid t)\\ \cdots\\ \eta(k+N_p\mid t)\end{bmatrix},\quad \psi_{k,t}=\begin{bmatrix}\widetilde{C}_{k,t}\widetilde{A}_{k,t}^{1}\\ \widetilde{C}_{k,t}\widetilde{A}_{k,t}^{2}\\ \widetilde{C}_{k,t}\widetilde{A}_{k,t}^{3}\\ \cdots\\ \widetilde{C}_{k,t}\widetilde{A}_{k,t}^{N_p}\end{bmatrix},$$

$$\Phi_{k,t}=\begin{bmatrix}\widetilde{C}_{k,t}\widetilde{B}_{k,t} & 0 & \cdots & 0\\ \widetilde{C}_{k,t}\widetilde{A}_{k,t}^{1}\widetilde{B}_{k,t} & \widetilde{C}_{k,t}\widetilde{B}_{k,t} & \cdots & 0\\ \widetilde{C}_{k,t}\widetilde{A}_{k,t}^{2}\widetilde{B}_{k,t} & \widetilde{C}_{k,t}\widetilde{A}_{k,t}^{1}\widetilde{B}_{k,t} & \cdots & 0\\ \cdots & \cdots & \cdots & \cdots\\ \widetilde{C}_{k,t}\widetilde{A}_{k,t}^{N_p-1}\widetilde{B}_{k,t} & \widetilde{C}_{k,t}\widetilde{A}_{k,t}^{N_p-2}\widetilde{B}_{k,t} & \cdots & \widetilde{C}_{k,t}\widetilde{B}_{k,t}\end{bmatrix},$$

$$\Delta u(k\mid t)=\begin{bmatrix}\Delta u(k\mid t)\\ \Delta u(k+1\mid t)\\ \Delta u(k+2\mid t)\\ \cdots\\ \Delta u(k+N_c\mid t)\end{bmatrix}.$$

b. Establishment of objective function

The goal of the controller is to eliminate the path-tacking errors of AHVs, and also to control the yaw angle. The objective function [17] is defined as:

$$\begin{aligned}&J(\xi(t),u(t-1),\Delta u(t))=\\ &\sum_{i=1}^{N_p}\left\|\eta(k+i\mid t)-\eta_{ref}(k+i\mid t)\right\|_Q^2+\\ &\sum_{i=1}^{N_c-1}\left\|\Delta u(k+i\mid t)\right\|_R^2+\rho\varepsilon^2\end{aligned} \tag{15}$$

where, η is the output vector, η_r is the reference vector, Q is a positive definite weighting matrix on system output, R is weighting parameter on the control input, ρ is the weight coefficient, and ε is the relaxation factor.

c. Determination of constraints

The AHVs can follow the target road quickly and accurately under the MPC control strategy. The MPC are subject to the following constraint conditions [18]:

$$\begin{aligned}&u_{\min}\le u\le u_{\max}\\ &\Delta u_{\min}\le \Delta u\le \Delta u_{\max}\\ &\varphi_{\min}\le\varphi\le\varphi_{\max}\\ &Y_{\min}\le Y\le Y_{\max}\end{aligned} \tag{16}$$

where, u_{min} and u_{max} are the limit values of the control input, Δu_{min} and Δu_{max} are the limit values of the control increment, φ_{min} and φ_{max} are the limit values of the yaw angle, and Y_{min} and Y_{max} are the limit values of the lateral position.

B. Design of optimal curvature preview control on straight road

When entering a straight line from a curve, the controller must reduce the path-tracking error while ensuring the stability in a straight line. The control strategy must be optimized to solve this problem, and the OCPC control strategy has a very good performance in the straight road driving. The OCPC preview time has an important effect on tracking performance. The longer the preview time, the longer the preview distance, the better the lateral stability of the vehicle. Thus, the lateral stability of the AHVs is improved, and the path-tracking performance is also enhanced [19] [20]. The dynamics characteristics of the AHVs under the OCPC is shown in Fig 5.

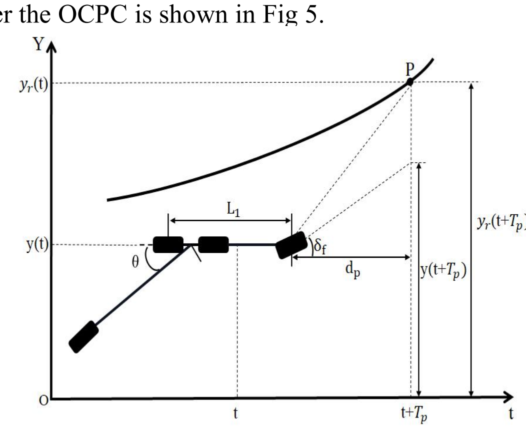

Fig 5. The Optimal curvature preview model of AHVs

According to Ackerman steering principle, we have

$$\tan\delta_f=\frac{L_1}{R} \tag{17}$$

According to the kinematic equation of circumferential movement of AHVs, the lateral acceleration is:

$$\ddot{y}=\frac{v_x^2}{R} \tag{18}$$

The driver previews the target position $y_r(t+T_p)$. After the preview time T_p passes, the lateral displacement of current position of AHVs is as follows:

$$y(t+T_p)=y(t)+\dot{y}(t)T_p+\frac{1}{2}\ddot{y}(t)T_p^2 \tag{19}$$

The preview distance at this point is:

$$d_p = v_x T_p \quad (20)$$

Assuming that the driver can control the tractor to reach the target position, from equations (17) to (20), the optimal wheel steering angle is:

$$\delta_f = \frac{2L}{d_p^{\,2}}(y_r(t+T_p) - y(t) - T_p \dot{y}(t)) \quad (21)$$

where, δ_f is the wheel steering angle, L_1 is the tractor axle distance, R is the steady-state turning radius, T_p is the preview time, and y(t) is the current position of the tractor.

IV. SIMULATION RESULTS

In order to compare and analyze the established path-tracking controller and MacAdam's optimal preview control (OPC), the Double Lane-Change Test by ISO 3888 [21] is used as the reference path, and the test speed is respectively 30km/h and 50km/h, and the Single Lane-Change Test by ISO 14791 [22][23] is used as the reference path, and the test speed is respectively 100km/h, to verify the road following and lateral stability of AHVs. The evaluation index of the road tracking ability is the lateral tracking error, the smaller the error, the better the road tracking ability. The lateral stability for the AHVs is often evaluated using rearward amplification (RWA), it is a ratio of the trailer's maximal yaw rate or lateral acceleration to the tractor's maximal yaw rate or lateral acceleration. If the RWA is less than 1, the lateral stability is better for the AHVs. Table 2 lists the controller parameters and values.

Table 2: Controller parameters and values

	Symbol	The value of 30 km/h	The value of 50 km/h	The value of 100 km/h
OCPC	T_p(s)	0.2	0.5	1
MPC	Np	30	20	40
	Nc	25	5	35
	Q	[2000,0; 0 10000]	[2000,0; 0 10000]	[2000,0; 0 10000]
	R	50000	50000	50000
	u(deg)	[-8,4.8]	[-8.8,2.62]	[-1.6,1.6]
	Δu(deg)	[-1.15,1.15]	[-1.72,1.72]	[-1,1]
	φ(deg)	[-14,9]	[-18,12]	[-3,5]
	Y(m)	[-2,4]	[-3,5]	[-1,3]

A. Characteristics analysis of different control strategies at low speed

In the model prediction controller, the reference lateral position and yaw angle of tractor under the Double Lane-Change are as follows:

$$Y_{ref}(X) = \frac{d_{y1}}{2}(1+\tanh(z1)) - \frac{d_{y2}}{2}(1+\tanh((z2))) \quad (22)$$

$$\varphi_{ref}(X) = \arctan(d_{y1}\cdot(\frac{1}{\cosh(z1)}))^2(\frac{1.2}{d_{x1}}) - d_{y2}\cdot(\frac{1}{\cosh(z1)})^2(\frac{1.2}{d_{x2}})) \quad (23)$$

where, d_{y1}=4.05, d_{y2}=5.7, d_{x1}=25, dx2=21.95, X_{s1}=27.19, X_{s2}=56.46.

$$z1 = \frac{2.4}{d_{x1}}(X - X_{s1}) - 1.2$$

$$z2 = \frac{2.4}{d_{x2}}(X - X_{s2}) - 1.2$$

Conditions: The vehicle speed is 30 km/h, μ=0.85. The simulation results of OPC and MPC+OCPC control strategies are shown and compared in Fig 6, and the error analysis is shown in Table 3.

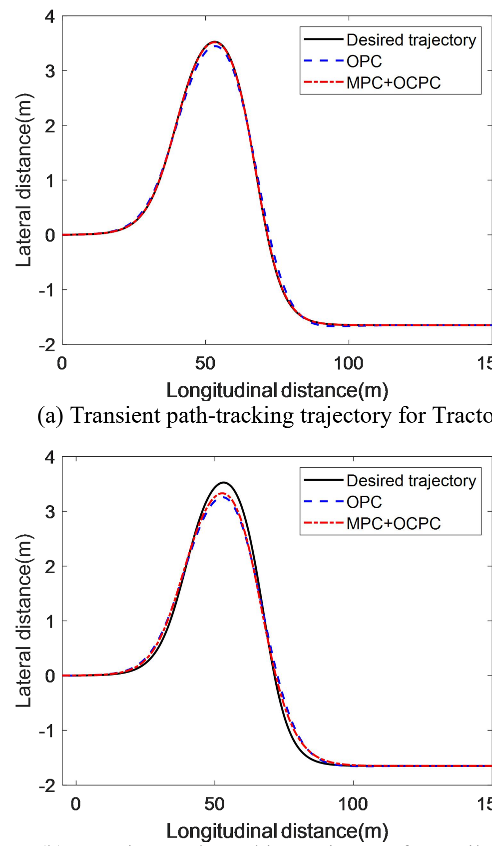

(a) Transient path-tracking trajectory for Tractor

(b) Transient path-tracking trajectory for Trailer

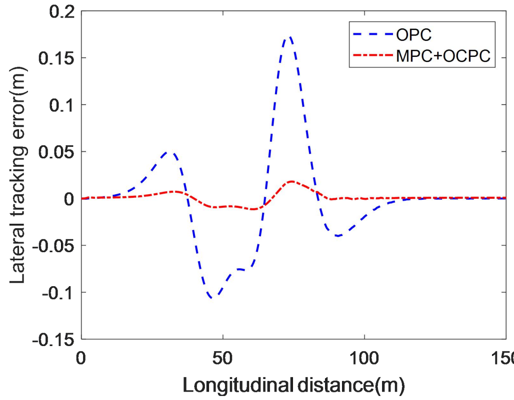

(c) Transient lateral errors relative to the desired trajectory

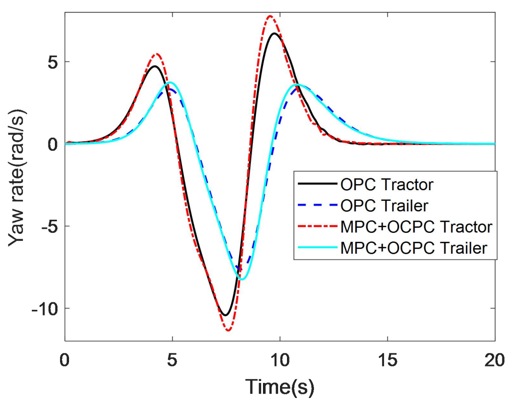

(d) Transient yaw rate

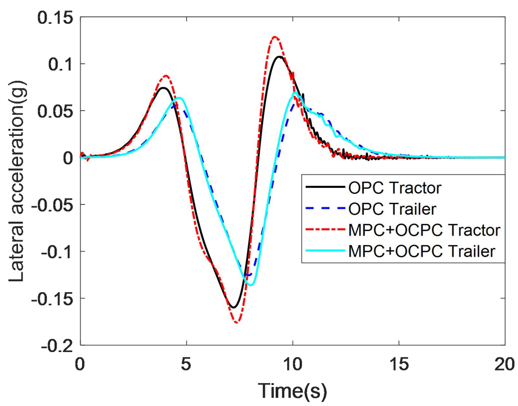

(e) Transient lateral acceleration

Fig 6. The transient characteristics of AHVs under the different control strategies and low speed condition

Table 3: Model comparison

	Max. trajectory error	Max. yaw rate	Max. lateral acceleration
OPC	17 cm	10.43 deg/s	1.47 m/s^2
MPC+OCPC	3cm	11.35 deg/s	1.67 m/s^2
The improvement of MPC+OCPC over OPC	↓14cm	↑0.92deg/s	↑0.2m/s^2

The simulation results in Fig. 6 show the path-tracking trajectories of the tractor and the trailer, the lateral tracking error, the yaw rate and the lateral acceleration. Analysis shows that the MPC+OCPC has the best road tracking performance in curved and straight segment, which is greatly improved compared with OPC. The maximum lateral tracking error is reduced by 14cm compared to OPC. It can be obtained from Fig 6(d) to Fig 6(e) that the ratio of the absolute peak yaw rate and lateral acceleration of the trailer to the tractor by the OPC and MPC+OCPC control methods is less than 1. The maximum ω ratio of OPC is 0.73, and the ratio of a_y is 0.81; the ω ratio of MPC+OCPC is 0.72, and the ratio of ay is 0.8. As shown in Table 3, the maximal yaw rate of the MPC+OCPC is only increased by 0.92 deg/s in comparison with the OPC, and the absolute value of the lateral acceleration is only increased by 0.2m/s^2 in comparison with the OPC, the overall performances of the AHVs are significantly improved by the MPC+OCPC designed in this paper.

B. Characteristics analysis of different control strategies at middle speed

Conditions: The vehicle speed sets to 50 km/h, μ=0.85.The simulation results of OPC and MPC+OCPC control strategies are shown and compared in Fig 7, and the error analysis is shown in Table 4.

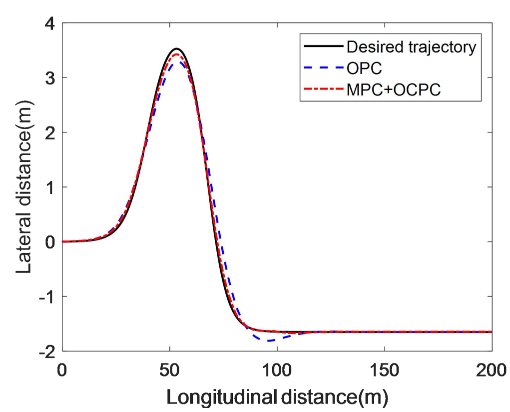

(a) Transient path-tracking trajectory of Tractor

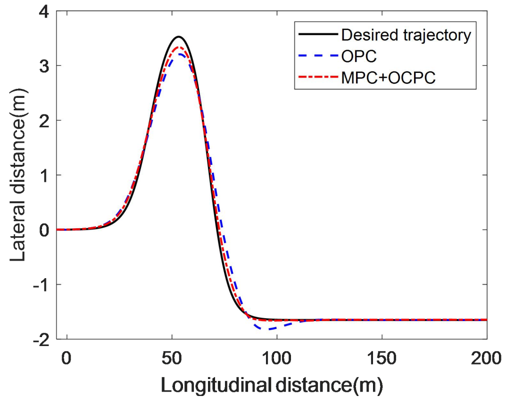

(b) Transient path-tracking trajectory of Trailer

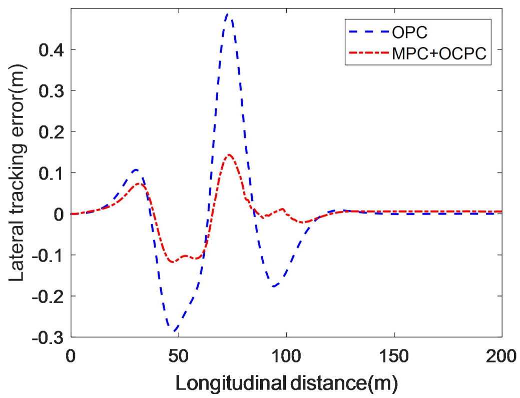

(c) Path-tracking error relative to the desired trajectory

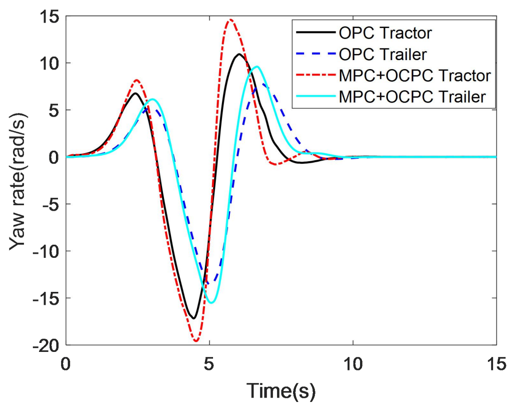

(d) Transient yaw rate

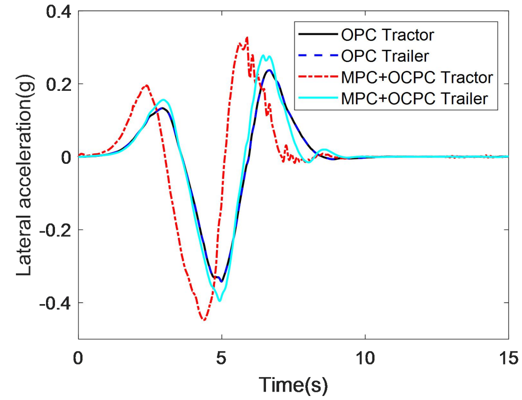

(e) Transient lateral acceleration

Fig 6. The transient characteristics of AHVs under the different control strategies and middle speed condition

Table 4: Model comparison

	Max. trajectory error	Max. yaw rate	Max. lateral acceleration
OPC	49 cm	17.16 deg/s	3.76m/s^2
MPC+OCPC	13 cm	19.58deg/s	3.92 m/s^2
The improvement of MPC+OCPC over OPC	↓36cm	↑2.42deg/s	↑0.16m/s^2

As in Fig. 7, the simulation results show the trajectory of the tractor and the trailer, the lateral tracking error, the yaw rate and the lateral acceleration. MPC+OCPC aims to reduce the lateral error in the curve segment, and the road tracking effect is good, and the lateral tracking error of MPC+OCPC is greatly reduced compared with OPC; in the straight segment, stable driving is the goal, and the stability is also better. It can be obtained from Fig 7(d) to Fig 7 (e) that the ratio of the maximal yaw rate and the lateral acceleration of the trailer to the tractor is less than 1. The maximal ratio ω of the MPC+OCPC is 0.79, and the maximal ω of the OPC is 0.79, and the lateral stability is great. However, it can be seen from Fig 7(a) to Fig 7(c) that the MPC+OCPC is closer to the target trajectory in the curve and straight segments than the OPC. And it can be obtained from Table 4 that the maximal lateral error of the MPC+OCPC is 36cm and smaller than the OPC, which greatly improves the path-tracking ability.

C. Characteristics analysis of different control strategies at high speed

In the model prediction controller, the reference lateral position and yaw angle of tractor under the Single Lane-Change are as follows:

$$Y_{ref}(X) = \frac{d_y}{2}(1+\tanh(z)) \tag{24}$$

$$\varphi_{ref}(X) = \arctan(d_y \cdot (\frac{1}{\cosh(z)}))^2 (\frac{1.2}{d_x})) \quad (25)$$

where, d_y=1.46, d_x=25, X_s=30.5.

$$z = \frac{2.4}{d_x}(X - X_s) - 1.2$$

Conditions: The vehicle speed sets to 100 km/h, μ=0.85. The simulation results of OPC and MPC+OCPC control strategies are shown and compared in Fig 8, and the RWA analysis is shown in Table 5.

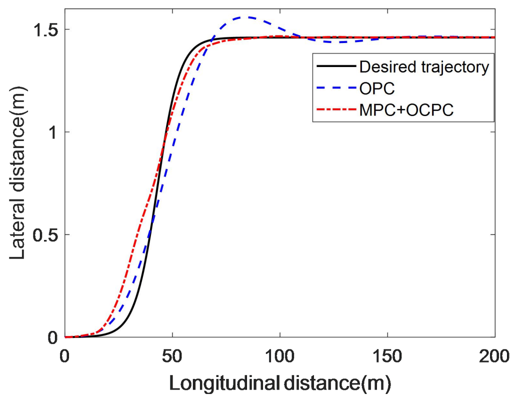

(a) Transient path-tracking trajectory for Tractor

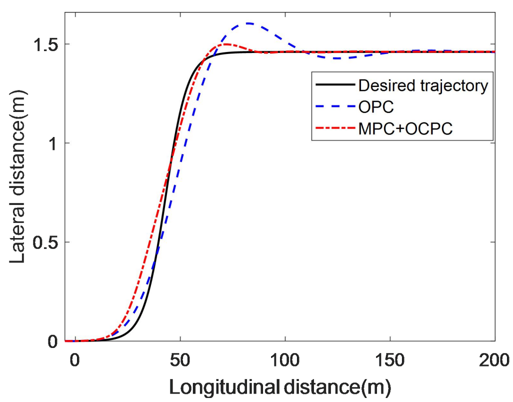

(b) Transient path-tracking trajectory for Trailer

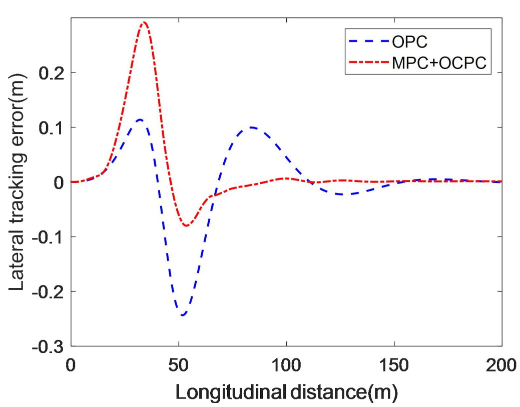

(c) Transient lateral errors relative to the desired trajectory

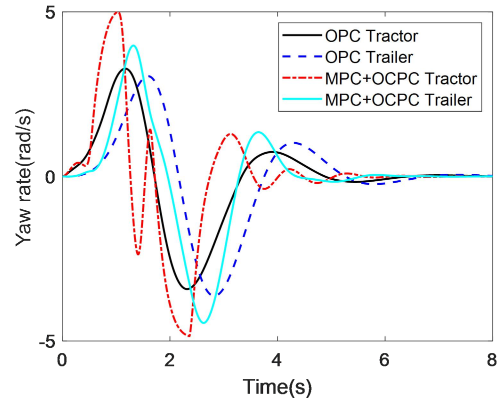

(d) Transient yaw rate

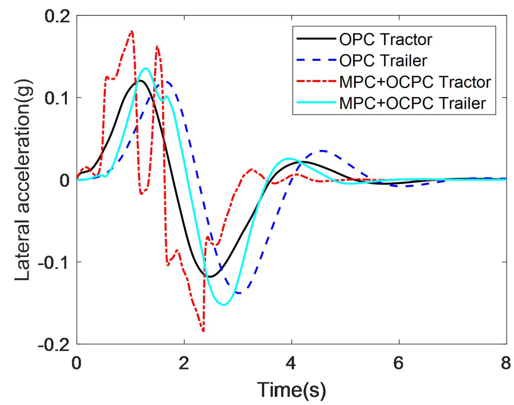

(e) Transient lateral acceleration

Fig 8. The transient characteristics of AHVs under the different control strategies and high speed condition

Table 5: RWA comparison

	OPC	MPC+OCPC
$\lvert\omega_{1max}\rvert$	3.42 deg/s	5 deg/s
$\lvert\omega_{2max}\rvert$	3.63 deg/s	4.45 deg/s
$\lvert a_{y1max}\rvert$	0.12 m/s^2	0.18 m/s^2
$\lvert a_{y2max}\rvert$	0.14 m/s^2	0.15 m/s^2
ω RWA	1.06	0.89
a_y RWA	1.17	0.83

As in Fig. 8, the simulation results show the trajectory of the tractor and the trailer, the lateral tracking error, the yaw rate and the lateral acceleration. The MPC+OCPC turns in advance at the beginning of Single Lane-Change, the path-tracking effect is worse than OPC, the maximum tracking error is 29cm, but the path-tracking is great at the ending of Single Line Change. The OPC path-tracking cuve fluctuates greatly at the ending of Single Line-Change, and the path-tracking effect is poor. The maximum tracking error is 25cm, and the AHVs become unstable. When AHVs are traveling at high speed, the RWA as the main evaluation index. It can be obtained from Table 5 that the RWA of yaw rate and lateral acceleration of OPC is more than 1. The ω RWA of the OPC is 1.06 and the a_y RWA of OPC is 1.17, and the lateral stability is terrible. However, it can be seen that the RWA of yaw rate and lateral acceleration of the MPC+OCPC is less than 1. The ω RWA of the MPC+OCPC is 0.89, and the a_y RWA of the MPC+OCPC is 0.83, which greatly improves the lateral stability. In summary, the MPC+OCPC is superior to the MacAdam's OPC in the road-followability and lateral stability of the AHVs.

V. CONCLUSIONS

Aiming at the path-following problem of the AHVs, a new path-tracking controller is proposed base on the MPC method and the OCPC technique. Based on the vehicle dynamic model of AHVs, a combined path-tracking controller is established. The controller inherits the advantage of the MPC in the curve segment and the benefit of the OCPC in the straight segment, and separately to improve the path-tracking ability in curve segment by the MPC control strategy and to enhance the driving stability in straight line segment by the optimal curvature preview controller of AHVs. The simulation results show that the new path-tracking controller can effectively follow the target route in the comprehensive road segment and the driving stability of AHVs has also improved significantly.

REFERENCES

[1] Jinghua Guo, Keqiang Li, et al: Review of Research on Intelligent Vehicle Motion Control[J]. Journal of Automotive Safety and Energy, 2016, 7(2) : 151-159.

[2] A. Amir, Y. He: A Review of Essential Technologies for Autonomous and Semi-Autonomous Articulated Heavy Vehicles. Proceedings of the Canadian Society for Mechanical Engineering International Congress 2020, June 21-24, 2020, Charlottetown, PE, Canada, 8 pages.

[3] C.C.MacAdam：An Optimal Preview Control for Linear Systems[J]. Journal of Dynamic Systems Measurement & Control，1980，102(3)：188-190.

[4] C.C.MacAdam：Application of an Optimal Preview Control for Simulation of Closed-loop Automobile Driving[J]. IEEE Transactions on Systems，Man and Cyberbetics，1981，11(6)：393-399.

[5] A.Y.Ungoren and H.Peng：An adaptive lateral preview drive model[J], Vehicle System Dynamic, 2005, vol43, 245-259.

[6] X. Ding, Y. He: Numerical Simulation and Analysis of Closed-Loop Driver/ Articulated Vehicle Dynamic System. SAE Int. J. Commer. Veh. 2012, 5(1): 111-118, 2012, https://doi.org/10.4271/2012-01-0244.

[7] S. Zhu, Y. He: A Unified Lateral Preview Driver Model for Road Vehicles. IEEE Transactions on Intelligent Transportation Systems, 2020, Vol. 21, No. 11, 4858-4868.

[8] Paolo Falcone, H.Eric Tseng and Francesco Borrelli：MPC-based Yaw and Lateral Stabilisation via Active Front Steering and Braking[J], Vehicle System Dynamic, 2008, vol46：611-628.

[9] D.Hodo：Development of an Autonomous Mobile Robot-trailer System for UXO detection. Master’s thesis，Auburn University，2007.

[10] J.T.Salmon：Guidance of an Off-road Tractor-trailer System Using Model Predictive Control.. Master’s thesis, Auburn University, 2013.

[11] Wu T and Hung J Y：Path Following for a Tractor-trailer System Using Model Predictive Control[C]. IEEE，Southeastcon，2017.

[12] Pan K, Zheng H and Wu J：Research on the Control Strategy of Trailer Tracking Tractor for Articulated Heavy Vehicles. SAE Technical Paper, 2019.

[13] M.M. Islam, Y. He, S. Zhu, Q. Wang: A Comparative Study of Multi-Trailer Articulated Heavy-Vehicle Models. Proceedings of the Institution of Mechanical Engineers, Part D: Journal of Automobile Engineering, 2015, Vol.229, No. 9, pp.1200-1228.

[14] Xu T, Ji X, Liu Y , et al：Differential Drive Based Yaw Stabilization Using MPC for Distributed-drive Articulated Heavy Vehicle[J]. IEEE Access，2020.

[15] Lefèvre，Stéphanie，Carvalho A，Gao Y，et al：Driver Models for Personalised Driving Assistance[J]. Vehicle System Dynamics，2015:1705-1720.

[16] Yan Zhang，Miaohua Huang：Path following control of intelligent driving vehicle based on model predictive control[J]. Journal of Digital Manufacturing Science, 2019, 17(01):25-30.

[17] Bai G，Meng Y，Liu L，et al. A New Path Tracking Method Based on Multilayer Model Predictive Control[J]. Applied Sciences, 2019, 9(13):2649.

[18] Goorts K，Narasimhan S：Model Predictive Control for Deployable, Autonomous Control Systems[C]. The 7th World Conference on Structural Control and Monitoring，2018.

[19] Konghui Guo: Preview Optimal Curvature Model of Driver-Car Closed-loop System Maneuvering Movement[J]. Journal of Automotive Engineering，1984(03)：3

[20] Xin Guan, Yongshang Chen, et al: Composite correction of preview following driver model[J]. Journal of Automotive Engineering，2018，040(003)：297-304.

[21] Yiqi Gao：Model Predictive Control for Autonomous and Semiautonomous Vehicles[D]. University of California，Berkeley，2014.

[22] Q. Wang, Y. He: A Study on Single Lane-Change Manoeuvres for Determining Rearward Amplification of Multi-Trailer Articulated Heavy Vehicles with Active Trailer Steering Systems. Vehicle System Dynamics, 2016, Vol. 54, No. 1, pp.102-123.

[23] Z. Ni, S. Zhu, Y. He: A Comparison of Test Manoeuvres for Determining Rearward Amplification of Articulated Heavy Vehicles. International Journal of Heavy Vehicle Systems, 2020, Vol. 27, No. 4, 405-421.